Parasitol Res (2015) 114:37–45
DOI 10.1007/s00436-014-4157-5

ORIGINAL PAPER

Thelohanellus wangi n. sp. (Myxozoa, Myxosporea), a new gill parasite of allogynogenetic gibel carp (*Carassius auratus gibelio* Bloch) in China, causing severe gill myxosporidiosis

S. Yuan · B. W. Xi · J. G. Wang · J. Xie · J. Y. Zhang

Received: 25 June 2014 / Accepted: 23 September 2014 / Published online: 7 October 2014

Abstract We describe here a new myxozoan, *Thelohanellus wangi* n. sp., infecting the allogynogenetic gibel carp, *Carassius auratus gibelio* (Bloch), in a fry nursery farm in Jiangsu Province, China. Polysporous gray white round or ovoid plasmodia, 500–1,500 μm in size, were found exclusively in the gill filaments. The diagnostic characteristics of the myxospores are as follows: spore melon seed shaped in frontal view with smooth surface and asymmetrical valves; convex-shaped in sutural view with straight or slightly bent and thick sutural line, averaging 20.2 (16.5–22.3)×9.9 (9.1–10.8)×9.3 μm (8.2–10.4) in size; and one elliptical polar capsules with subulate anterior end and round posterior end, averaging 10.1 (8.4–11.2)×6.5 μm (6.1–7.0) in size. Polar filaments coil six to seven turns and are slightly oblique to the longitudinal axis of the polar capsule. An elongate melon seed-shaped mucus envelope surrounds almost completely the spore, but with largest distance in posterior end between spore valve and mucus envelope. Granular sporoplasm contains two slightly oval nuclei, and no iodinophilous vacuole is observed. Histopathological analysis showed that the plasmodia embedded in the gill filaments and occasionally extended into the connective tissue of the gill arch. No significant inflammatory responses were provoked by the infection. The development of parasite is asynchronous, with mature spores centrally locating and trophozoites and pre-sporogonic stages peripherally locating within the plasmodia. Overall prevalence was 74 % (37/50). Infection intensity was usually high, with about 10–30 cysts per fish. Phylogenetical analysis shows that *T. wangi* n. sp. is most closely related to several *Thelohanellus* species infecting cyprinid fish and formed a *Thelohanellus* clade based on the ribosomal DNA data. The cysts of this myxosporean were only found from fry seed with body length below 7 cm, generally from late April to early June when the fry fish of allogynogenetic gibel carp were nursed in the epizootic areas.

Keywords *Thelohanellus wangi* n. sp. · Allogynogenetic gibel carp · Histopathology · Morphology · Phylogeny

Introduction

Allogynogenetic gibel carp, *Carassius auratus gibelio* (Bloch), has been becoming one of the most popular freshwater cultured species with commercially importance in the mainland of China since it was selectively bred by its special dual reproduction modes of gynogenesis and syngenesis in the early 1980s (Gui and Zhou 2010). With the improvement of intensive aquaculture techniques and production of a new variety, designated as the allogynogenetic gibel carp "CAS III," this species has been widely extended for culture into many freshwater wetlands, and the annual production capacity was up to 2 million tons in 2011 in China (Wang et al. 2011). Meanwhile, accompanied with the rapid development of allogynogenetic gibel carp aquaculture industry, more and more pathogenic organisms have been reported to cause morbidity, mortality, and severe economic losses (Luo et al. 2013). Among them, myxozoans represent an important parasitic group (Wang et al. 2001; Zhang et al. 2010a, b; Xi et al. 2011). Furthermore, frequent transregional trade of

S. Yuan and B. W. Xi contributed equally to this work.

S. Yuan · J. G. Wang · J. Y. Zhang (✉)
Fish Diseases Laboratory, State Key Laboratory of Freshwater Ecology and Biotechnology, Institute of Hydrobiology, Chinese Academy of Sciences, 430072 Wuhan, China
e-mail: zhangjy@ihb.ac.cn

S. Yuan
Jiangsu Agri-Animal Husbandry Vocational College, 225300 Taizhou, Jiangsu, China

B. W. Xi · J. Xie
Freshwater Fisheries Research Center, Chinese Academy of Fishery Sciences, 214081 Wuxi, Jiangsu, China

seedlings and marketable fish under the condition of lacking strict quarantine further accelerated the transmission of these agents in China, and some wild fish in the epizootic were found to be infected by myxosporean spilled from cultured allogynogenetic gibel carp (authors' unpublished data). Reducing the severe negative effects of the myxosporidiosis on this commercially important species has been considered a priority in China. Until now, more than 40 myxosporean species belonging to *Myxobolus*, *Thelohanellus*, *Hennegua*, *Sphaerospora*, *Myxidium*, *Myxobilatus*, *Hoferellus*, *Chloromyxum*, *Zschokkella* and *Unicauda* genera have been found in allogynogenetic gibel carp, with high diversity of infection habitats (Xiao 1988; Chen and Ma 1998; Zhang et al. 2006; Zhao et al. 2008; Zhang et al. 2010a, b; Liu et al. 2012; Zhao et al. 2013; Liu et al. 2014a, b; Ye et al. 2014). These myxosporean parasites can infect almost all stages of a whole culture cycle of this fish. Some of them show high bias of infection to fish size. For instance, *Thelohanellus wuhanensis* exclusively infects the fry of nursery stage, but *Myxobolus turpisrotundus*, *Myxobolus honghuensis*, and *Myxobolus ampullicapsulatus* are obligate parasites of the fattening fish (Wang et al. 2001; Zhang et al. 2010b; Xi et al. 2011; Liu et al. 2012).

In northern Jiangsu province, East China, there is more than 50,000 ha of intensive culture area for allogynogenetic gibel carp which is one of the biggest culture regions in China. Most of reported myxosporeans infecting allogynogenetic gibel carp can be found in this area, and myxosporidiosis represents top threats among the list of diseases (Xi et al. 2011; Luo et al. 2013). The estimated annual economic losses caused by the infection of myxosporeans in the local cultured allogynogenetic gibel carp exceed ¥100 million (Xi et al. 2011). To obtain thorough information of myxosporean fauna in cultured allogynogenetic gibel carp in this area, we conducted a comprehensive parasitological investigation for two successive years, concentrating on the stages of seed breeding and fattening. As a partial work of this investigation, a new *Thelohanellus* species, found in the gill filaments of allogynogenetic gibel carp, is herein described with morphological, histopathological, and molecular data.

Materials and methods

Allogynogenetic gibel carp (3–6-cm total length) from a commercial nursery farm in Sheyang country, northern Jiangsu province of China, were sampled for diagnosis of large amounts of myxosporean cysts in the gills, and occurrence of mass mortality was previously reported by the local fishery technicians. Fifty individual fish were randomly selected and transported alive to the laboratory for the parasitological examination. Preliminary observation by light microscopy showed that the cysts dwelling in the gills were myxosporean plasmodia and the unknown species belonged to *Thelohanellus* genus. The clinical symptoms and disease history were documented in the field. Infected gill tissues, containing the plasmodia, liver, spleen, and other internal organs, were preserved in 10 % neutral buffered formalin for histopathological analysis and the isolated plasmodia in 95 % ethanol for extracting the genomic DNA.

Morphological and histological examination

Individual cyst of the tentatively identified *Thelohanellus* sp. (n= 6) was placed on a microscope slide and mechanically ruptured to make a wet mount with a drop of physiological saline (0.85 % of NaCl, *w*/*v*). Morphological and morphometrical features of spores were characterized according to Lom and Arthur (1989) by measuring 60 mature spores from three different plasmodia in the wet preparation. Measurements of spores were performed using an Olympus BX53 microscope equipped with an ocular micrometer. Lugol's iodine (2 %) was used to visualize iodinophilic vacuole. Spores were photographed with the use of Zeiss Axioplan 2 Image and Axiophot 2 with differential interference contrast lens. Line drawings were made based on the taken photographs with the aid of CorelDRAW X5 (Corel, Ottawa, Canada) and Adobe Illustrator software (Adobe Systems, San Jose, CA, USA). All measurements are given as means (range) in micrometers (μm) unless otherwise stated. For histopathological analysis, formalin-fixed infected gill tissues containing plasmodia were dehydrated and embedded in paraffin wax. Sections cut at 5–6 μm were stained with hematoxylin and eosin (H & E) and observed under light microscopy.

DNA isolation and sequencing

Genomic DNA (gDNA) was extracted from plasmodia isolated from ethanol-preserved samples. Three individual plasmodia from the different infected fish were used to confirm the congruence of DNA sequences. The parasite gDNA were isolated by proteinase K digestion for 4 h at 56 °C with several interval vortex agitations. After confirming the digestion effects by light microscopy, the homogenate solution was extracted by phenol-chloroform and precipitated by ethanol. The purified gDNA was then suspended in 120 μl of double-distilled water and stored at −20 °C. Partial sequences of small subunit (SSU) ribosomal DNA (rDNA) were amplified by polymerase chain reaction (PCR) with the primer pair, MyxospecF-18R (Fiala 2006). The 50-μl reaction mixture contained approximately 200 ng of extracted gDNA, 5 μl of Takara Taq Hot Start Version 10× PCR buffer (Takara Bio, Dalian), 5 mM of each deoxyribonucleotide triphosphate, 20 pmol of each primer, 1 U of Takara Taq Hot Start Taq polymerase, and nuclease-free water to the volume. The reaction mixture was cycled on a Bio-Rad PTC-100 Thermocycler. The following temperature profile was used: preheating at 95 °C for 5 min, 35 cycles of denaturation at

94 °C for 1 min, annealing at 46 °C for 50 s and extension 65 °C for 90 s, and a further elongation step at 65 °C for 10 min. PCR products were gel-excised and purified using a QIA quick gel extraction kit (QIAGEN). Purified PCR products were sequenced in both directions using the ABI PRISM® 3730 DNA sequencer (Applied Biosystems, Foster City, CA, USA). The sequencing primers were as same as the PCR primers. The obtained forward and reverse sequence segments were assembled using the SeqMan utility of the Lasergene software package (DNASTAR, Madison, Wisconsin), and sequence ambiguities were clarified using corresponding ABI chromatograms by eyes. The resulting sequences were compared with related rDNA sequences available in GenBank using BLAST to confirm if it was the SSU ribosomal RNA (rRNA) gene of myxozoans and submitted to GenBank with accession number JX458816.

Phylogenetic analysis

Selected myxozoan SSU rRNA gene sequences were aligned with Clustal X (Thompson et al. 1997) using default settings. Phylogenetic analysis of aligned sequences, excluding the gaps, was conducted by the neighbor-joining (NJ) method, the maximum parsimony (MP) method, the maximum likelihood (ML), and the Bayesian method which were implemented in the MEGA5 computer package (Tamura et al. 2011), PAUP* 4.0b1 (Swofford 2003), and PhyML (Guindon et al. 2010), respectively. Parsimony analysis used the heuristic search algorithm and tree bisection-reconnection (TBR) branch swapping. Bootstrap values were calculated with 1,000 replicates using the heuristic search algorithm and TBR branch swapping. NJ analysis of genetic distances was calculated with Kimura 2 model parameter (Kimura 1980) to construct a NJ tree. Optimal evolutionary models for ML and Bayesian analysis were selected by jModelTest using the Akaike information criteria and identified as the general time reversible model (GTR + I + G) (Posada 2008). Nucleotide frequencies were estimated from the data (A=0.2759, C=0.175; G=0.2652, T=0.3019), and six rates of nucleotide substitution were [AC]=1.0000, [AG]=3.7913, [AT]=1.0000, [CG]=1.0000, [CT]=6.1766, and [GT]=1.0000. Bootstrap support values were calculated with 1,000 replicates. Trees were initially examined in TreeView X (Page 1996) and edited and annotated in Adobe Illustrator.

Results

The infected fish were always grasping at the water surface, even though under sufficient dissolved oxygen (DO). Among the sampled 50 specimens, 37 (74 %) had plasmodia of the undetermined parasite belonging to the genus *Thelohanellus*. The highest prevalence, however, could be up to 100 % about 10 days ago before this sampling, according to the observation of the farmer and local technicians. The usage of insecticides can partly explain the decrease of prevalence. Most of the examined plasmodia contained only mature spores, and few pre-sporogonic stages could be observed in some wet preparations, indicating late infection stage of this species. The myxosporean exclusively colonized in the gills, and no plasmodia and spores could be found in other organs. Some plasmodia remnants could be seen in the gills of the restored fish after plasmodia shedding. In addition, some *Trichodina nobilis* could be found in the gill filaments of the examined fish, but both the infection prevalence and intensity are low.

Thelohanellus wangi n. sp.

Based on the strictly morphological comparison, this gill-dwelling myxosporean can be concluded to be a new species and designated as *T. wangi* n. sp.

Description The plasmodia are polysporic, gray white, and round or ovoid and measured 500–1,500 μm in size (Fig. 1). The histopathological analysis showed that the parasite develops in the gill filaments and the plasmodia almost destroyed and displaced the infected gill filaments and neighbor filaments. The plasmodia belong to intrafilamental-cartilage type (type II, plasmodia in the gill filaments) according to the Molnár's classification regarding myxosporean plasmodia in different areas of fish gills (Molnár 2002). The basal parts of the plasmodia connected with cartilage of gill arch and the anterior part extend to the terminal end of the filaments where obvious epithelial hyperplasia could be found (Fig. 2a, b). It was occasionally found that large plasmodia were formed by fusion of several neighbor extended plasmodia (Fig. 2a). Other filaments were not severely affected. The mature spores, with subulate anterior end and round

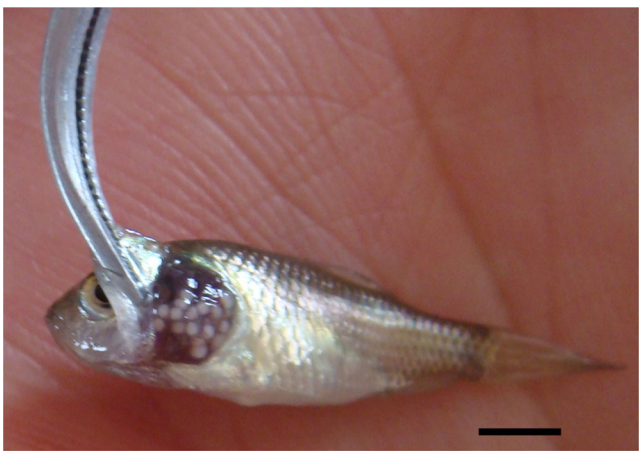

Fig. 1 Allogynogenetic gibel carp, *Carassius auratus gibelio* Bloch, heavily infected with *Thelohanellus wangi* n. sp. in the gills, showing visible cysts. *Scale bar*=0.5 cm

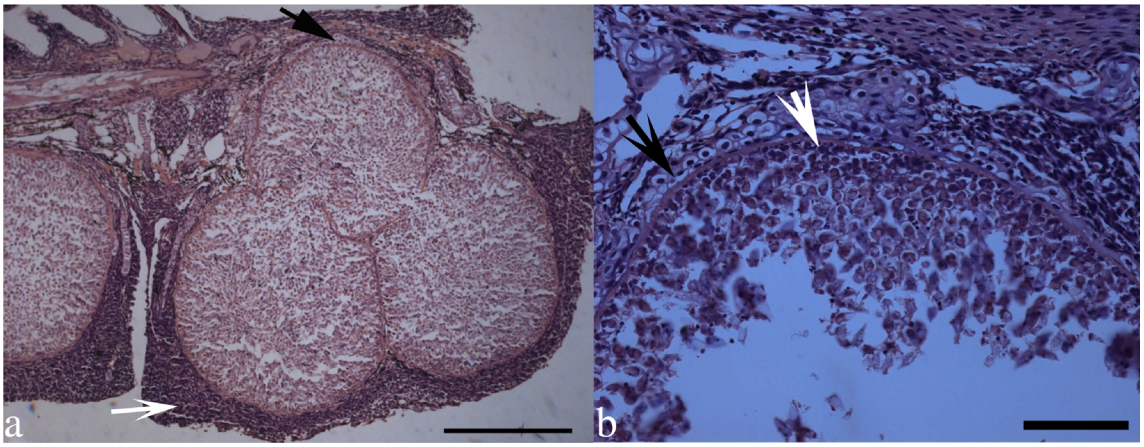

Fig. 2 Histological sections of infected gill filaments by *Thelohanellus wangi* n. sp. **a** A cyst was formed by fusing neighbor three plasmodia (many-to-one type) and extended into the connective tissue of the gill arch (*black arrow*). Note the obvious epithelial hyperplasia at the anterior part of the infected gill filaments. *Scale bar*=0.5 mm. **b** A cyst forming by a single plasmodium. Note the few pre-sporogonic stages at the periphery of plasmodium (*white arrow*) and the plasmodium delimited by a thin connective tissue membrane from cartilage cells of gill filaments (*black arrow*). *Scale bar*=100 μm

posterior end, were melon seed-shaped in frontal view and convex-shaped in sutural view, with a length ranging from 16.5 to 22.3 μm (average 20.2 μm). The width and thickness of mature spores ranged from 9.1 to 10.8 μm (average 9.9 μm) and 8.2 to 10.4 μm (average 9.3 μm), respectively (Fig. 3, Table 1). The spore wall was smooth, and the two spore valves were asymmetrical, with a conspicuous straight and thick sutural line. The ratio of spore length and width was above 2 (Figs. 3 and 4). One polar capsule, opening at the anterior part of spores, was elliptical, and the size was 10.1 μm (8.4–11.2) in length and 6.5 μm (6.1–7.0) in width. The polar capsule occupied more than half of the spores. The polar filaments were coiled six to seven turns and oblique to the polar capsule longitudinal axis. Polar filament was easily extruded after stimulation with potassium hydroxide or even with the pressure of coverslips. An elongate melon seed-shaped mucus envelope was remarkable for most of myxospores which surround almost completely the spore valves. The largest distance between spore valves and mucus envelope was found in posterior end of spores (Figs. 3 and 4a). Two slightly oval nuclei could be found in granular sporoplasm, but no iodinophilous vacuole was observed. Some deformed myxospores with two polar capsules, like *Myxobolus* spores, can occasionally found in plasmodia (Fig. 3c). Sporogenesis was asynchronous, with pre-mature developmental stages in the periphery and mature spores in the center of plasmodia.

Taxonomic summary of ***T. wangi*** n. sp.

Type host: *Carassius auratus gibelio* (Bloch)
Site of infection: gill filaments
Prevalence: 74 % (37/50)
Locality: Sheyang country, Jiangsu Province, China.
Type material: Syntype specimens of spores in glycerin gelatin and H & E-stained section deposited in the Laboratory of Fish Diseases, Institute of Hydrobiology, Chinese Academy of Sciences, accession no. MTR20120601. The partial 18S rDNA sequence was deposited in the GenBank under the accession number JX458816.

Etymology The species is named after Prof. Jianguo Wang, Institute of Hydrobiology, Chinese Academy of Sciences, in

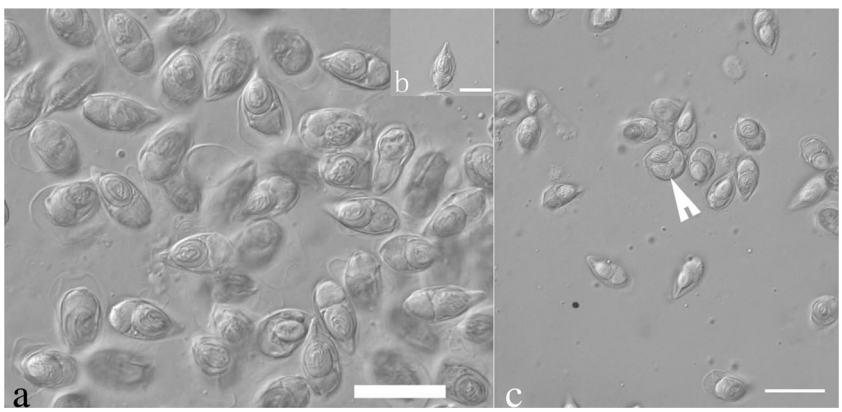

Fig. 3 Fresh myxospores of *Thelohanellus wangi* n. sp. **a** Myxospores in frontal view, *scale bar*=10 μm. **b** Myxospores in sutural view, *scale bar*=10 μm. **c** A deformed spore with two polar capsules (*white arrow*). *Scale bar*=20 μm

Table 1 Morphological comparison between *Thelohanellus wangi* n. sp. and the related species with similar morphological features

Species	LS (μm)	WS (μm)	TS (μm)	LPC (μm)	WPC (μm)	NC	DC (mm)	IS	References
Thelohanellus wangi n. sp.	20.2 (16.5–22.3)	9.9 (9.1–10.8)	9.3 (8.2–10.4)	10.1 (8.4–11.2)	6.5 (6.1–7.0)	6–7	0.5–1.5	Gill filaments	This study
T. nanhaiensis	17.0 (15.6–18.0)	10.0 (9.6–10.8)	7.8 (7.4–8.2)	8.9 (8.2–9.6)	5.1 (4.6–5.8)	6–7	ND	Gill	Chen and Ma (1998)
T. sagittarius	20.0 (19.2–20.6)	9.6 (8.0–10.2)	8.0 (ND)	10.6 (9.6–12.0)	7.2 (6.6–8.0)	8–9	0.06–0.08	Kidney, swim bladder, gill, Intestine etc.	Chen and Ma (1998)
T. parasagittarius	23.7 (22.8–24.6)	11.4 (10.2–12.0)	10.8 (ND)	12.1 (11.8–13.2)	8.3 (8.2–8.4)	6–7	ND	Skin, gill, gall bladder	Chen and Ma (1998)
T. nikolskii	19.2 (18.6–19.8)	10.7 (8.8–12.6)	9.3 (7.3–11.2)	7.8 (7.0–8.5)	5.3 (4.2–6.3)	6–8	0.5–3	Fins	Suo and Zhao (2010)
T. hovorkai	20.4 (18.0–22.4)	9.8 (7.2–12.0)	8.5 (7.0–10.0)	10.8 (7.2–14.4)	8.9 (7.2–10.8)	6–7	0.08–0.1	Gills, gall bladder, kidney	Chen and Ma (1998)
T. wuhanensis	23.6 (21–25)	13.8 (12.0–15.5)	11.7 (10.8–14.1)	11.5 (9.6–12.7)	9.1 (8.1–10.3)	8–10	0.5–1.7	Skin	Unpublished data
T. hokiangensis	23.9 (22.1–25.0)	10.7 (9.3–11.0)	10.7 (9.4–11.9)	13.4 (11.9–15.3)	9.2 (8.5–9.4)	6–7	0.025–0.036	Ureter, intestine	Chen and Ma (1998)
T. rhabdalestus	16.8±0.5	10.2±0.6	5.6±0.8	7.2±0.3	4.0±0.4	6–7	0.8	Liver, heart	Azevedo et al. (2011)

LS length of the spore, *WS* width of the spore, *TS* thickness of the spore, *LPC* length of the polar capsules, *WPC* width of the polar capsules, *PC* relative size of the polar capsules, *NC* number of coils of the polar filament, *DC* diameter of cysts, *IS* infected sites

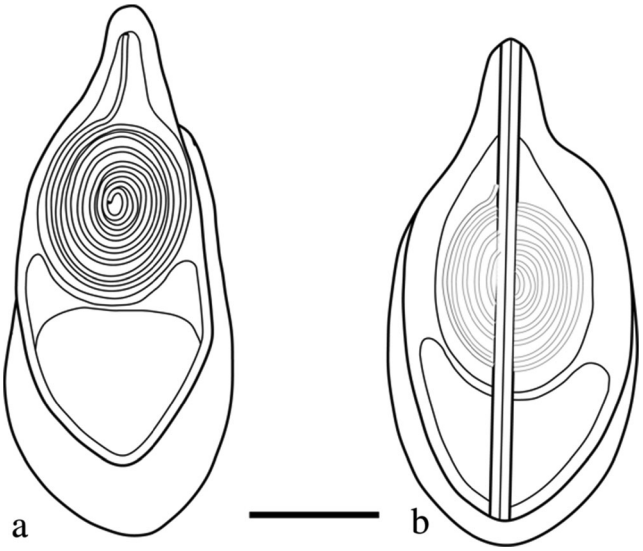

Fig. 4 Schematic drawings of myxospore of *Thelohanellus wangi* n. sp. **a** Frontal view. **b** Sutural view. *Scale bar*=5 μm

recognition of his significant contribution to the knowledge of fish parasitology, including freshwater myxosporeans in China.

Taxonomic remarks Out of approximately 109 species of the genus *Thelohanellus* (Zhang et al. 2013), *T. wangi* n. sp. displays a superficial similar morphological and morphometric charactertistics with *Thelohanellus nanhaiensis* Chen, 1998; *Thelohanellus sagittarius* Li et Nie, 1973; *Thelohanellus parasagittarius* Chen et Ma 1998; *Thelohanellus nikolskii* Akhmerov 1954; *Thelohanellus hovorkai* Akhmerov, 1960; *Thelohanellus wuhanensis* Xiao et Chen, 1993; *Thelohanellus hokiangensis* Ma, 1998; and *Thelohanellus rhabdalestus* Azevedo et al., 2011. However, the myxospore of *T. nanhaiensis* is slightly smaller than that of *T. wangi* n. sp.; especially, the ratio of spore length to spore width of the former is remarkably smaller than that of the latter. Additionally, the "S"-shaped sutural line of *T. nanhaiensis* can significantly differentiate it from the present species (straight sutural line). The ratio of polar capsule width to spore width of *T. sagittarius* and *T. parasagittarius* is obviously smaller than that of *T. wangi* n. sp. Further, the shape of polar capsule (pyriform) and coils of polar filament (8–9) of *T. sagittarius* also differ from *T. wangi* n. sp. with elliptical polar capsule and six to seven turns of polar filament. *T. nikolskii* can easily distinguish from *T. wangi* n. sp. by its elliptical spore and less 1/2 ratio of polar capsule length to spore length. Although the shape and size of polar capsule of *T. hovorkai* are almost identical with *T. wangi* n. sp., the former obviously differs from the latter by its coils of polar filaments (10–12 versus 6–7). The size, ratio of polar

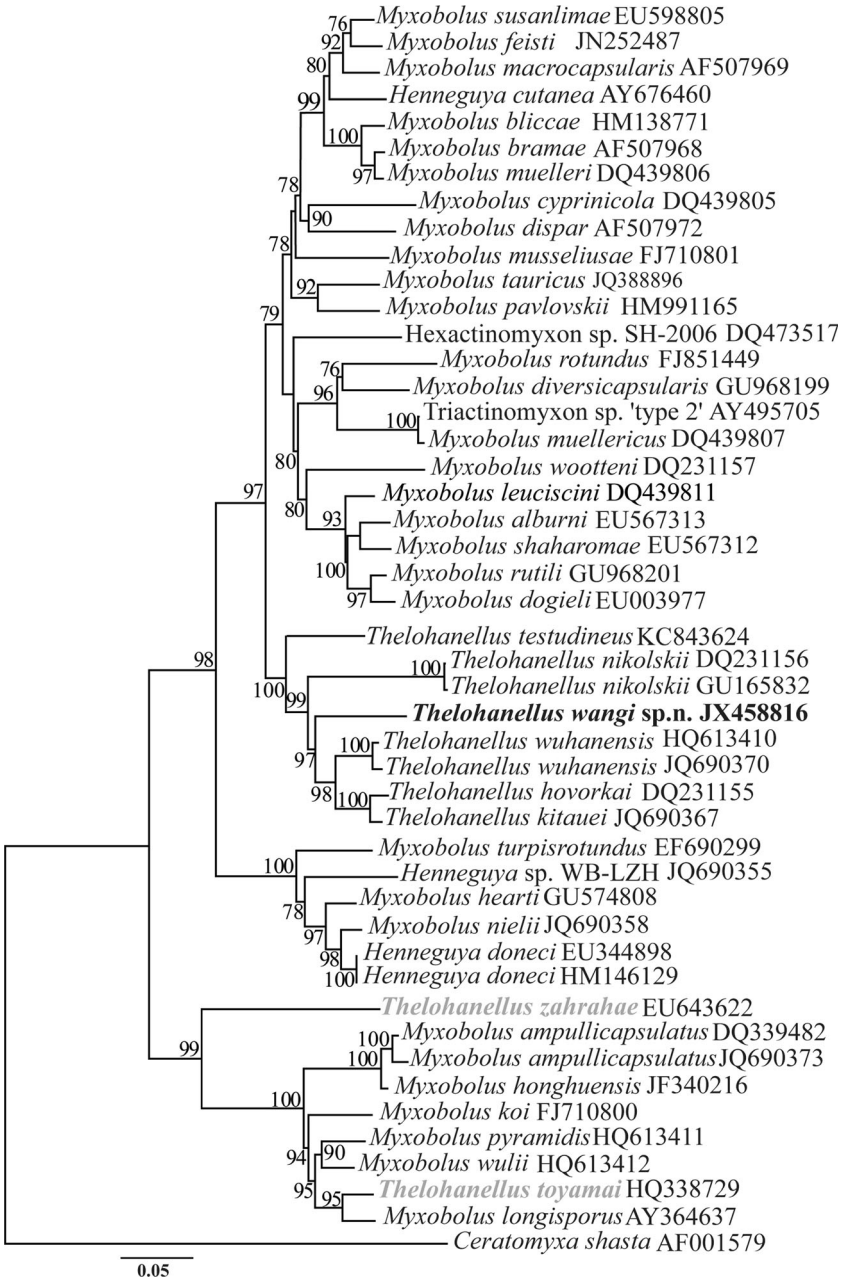

Fig. 5 Phylogenetic tree generated from maximum likelihood analysis of the aligned SSU rRNA gene sequences of *Thelohanellus wangi* n. sp. and selected species, with evolutionary model GTR + I + G. GenBank accession numbers are given adjacent to species names. *Numbers* at nodes indicate bootstrap confidence values (100 replications). *Thelohanellus wangi* n. sp. was highlighted by *bold black* and *T. zahrahae* and *T. toyamai* highlighted by *bold gray*

capsule length to spore length, and occurrence pattern of mucus envelope of *T. wuhanensis* are respectively different from those of *T. wangi* n. sp. The shape and size of *T. hokiangensis* polar capsules are respectively different from those of *T. wangi* n. sp. And also, the coiling pattern of polar filament of *T. hokiangensis* and *T. wangi* n. sp. is different (perpendicular Vs oblique to the longitudinal axis of the polar capsule). The pyriform spore, flask-shaped polar capsule, less 1/2 ratio of polar capsule length to spore length, infection site (liver and heart), and geographic distribution (India) make *T. rhabdalestus* easy to distinguish from *T. wangi* n. sp. Detailed morphological and morphometric comparisons between the present species and morphologically similar *Thelohanellus* species can be found in Table 1.

Phylogenetic analysis

A partial SSU rRNA gene with 1,659 bp in length was obtained after trimming the ambiguous positions in the two sequencing ends. Sequence analysis revealed that it was 92 % similar (1,510/1,636 bp) to *T. wuhanensis* from the skin of allogynogenetic gibel carp (JQ690370) and 92 % similar (1,035/1,126 bp) to *Thelohanellus testudineus* (KC843624) from the skin of allogynogenetic gibel carp, 91 % similar

(1,522/1,667 bp) to *Thelohanellus kitauei* reported from the intestine of common carp (JQ690367), 90 % similar (1,207/1,339 bp) to *T. hovorkai* reported from the mesentery of common carp, 89 % similar (1,459/1,637 bp) to *T. nikolskii* reported from the fins of common carp (GU165832), and then 88 % similar to *Myxobolus musseliusae* (1,452/1,643 bp) reported from the gills of common carp, respectively. Phylogenetic trees constructed by the applied three methods have similar topological structure although with different support values at some branch nodes. *T. wangi* n. sp. formed a sister relationship with the cluster of *T. wuhanensis*, *T. hovorkai*, and *T. kitauei* and then integrated *T. nikolskii* and *T. testudineus* to form an independent *Thelohanellus* clade with a high bootstrap support. The phylogenetic positions of *T. zahrahae* and *T. toyamai* are consistent to the previous reports, locating outside of the *Thelohanellus* clade (Fig. 5). *Thelohanellus sinensis* was not included in the present phylogenetic analysis for its short sequence length (less than 1,000 bp).

Discussion

Traditionally, the taxonomy of myxosporean parasites was largely based on the structure and shape of myxospores (Kent et al. 2001; Adriano et al. 2012). According to Lom and Dyková (2006), the myxospores of *Thelohanellus* species are generally tear-shaped or pyriform to broadly ellipsoidal in valvular view and more slender in sutural view, with always smooth spore valves usually surrounded by a mucous envelop and a single pyriform or a tear-shaped polar capsule harboring a single coil of polar filament. Based on these taxonomic features, about 109 *Thelohanellus* species have so far been described worldwide, which indicates that *Thelohanellus* is the sixth most speciose myxozoan genus after *Myxobolus*, *Myxidium*, *Henneguya, Ceratomyxa*, and *Chloromyxum* (Abdel-Ghaffar et al. 2013; Zhang et al. 2013). The described species here completely conforms to the morphological definition of *Thelohanellus* genus but differ morphologically from all described species, including all gill-dwelling and gibel carp-infecting species (please see the species description in "Results" section and Table 1). Moreover, molecular analysis also demonstrated that the sequence of the concerned species here did not match any subject in GenBank although only 12 species with molecular data are currently available. So, using the currently widely applied taxonomic synapomorphy for myxosporean parasites (spore morphology and molecular data, host and tissue tropism), it can be concluded that the present species is new to science and was designated as *T. wangi* n. sp.

Our phylogenetic analysis based on partial 18S rDNA sequences is consistent with several previous reports to support that *Thelohanellus* species have a close relationship with some *Myxobolus* species and *Thelohanellus* genus is a polyphyletic group with two species (*T. zahrahae* and *T. toyamai*) locating outside of the *Thelohanellus* clade (Kent et al. 2001; Székely et al. 2009; Griffin and Goodwin 2011; Liu et al. 2014a, b). A recent study showed that host specificity and infection site tropism were mostly correlated with the phylogeny among all biological features of Myxobolidae (Shin et al. 2014). However, two skin-infecting *Thelohanellus* species (*T. wuhanensis* and *Thelohanellus testudineus*) from allogynogenetic gibel carp did not form a direct sister group within the *Thelohanellus* clade in our and previous phylogenetic analysis (Zhu et al. 2012; Liu et al. 2014a, b; Shin et al. 2014). So, it still remains obscure to what extent the extant biological features of Myxobolidae represent the ancestor characters referred from their real phylogenetic relationships rather than 18S rDNA data-based phylogeny. Application of other molecular markers to construct phylogenetic tree and wide sampling for analysis can possibly solve these problems. Further considering *Thelohanellus* spp. evolved from an ancestor having two polar capsules at the anterior end and several times of possible loss and gain of polar capsules in the evolutionary history of *Thelohanellus* species (Bartosova et al. 2009; Liu et al. 2014a, b), it can be speculated that the extant different clades of *Thelohanellus* species evolved from different ancestors at different time points. Also, mucus envelope occurs in some myxospores of all species except *T. nikolskii* and *T. testudineus* within the main *Thelohanellus* clade but is absent for all species outside of the *Thelohanellus* clade, including *T. toyamai*, *T. zahrahae*, and *T. sinensis* (Chen and Ma 1998; Yokoyama et al. 1998; Székely et al. 2009; Suo and Zhao 2010; Griffin and Goodwin 2011; Zhu et al. 2012; Liu et al. 2014a, b). So, several times of possible loss and gain of mucus envelop probably occurred during the evolution of *Thelohanellus* species. However, the possible role of mucus envelope remains unknown, and its possible role to referring the phylogenetic relationships of interspecies within *Thelohanellus* genus awaits more data to support. Additionally, sequence data of most of *Thelohanellus* species are unavailable to impede the further analysis.

Histological analysis showed that cyst of *T. wangi* n. sp. generally formed by a single plasmodium (one-to-one type), but some cysts occasionally formed by integrating several neighbor small plasmodia, belonging to many-to-one type suggested by Liu et al. (2014a, b). However, unlike *Myxobolus wulii* (Zhang et al. 2010b) and *T. testudineus* (Liu et al. 2014a, b), these many-to-one type cysts of *T. wangi* n. sp. were generally produced by joining two or three plasmodium. Whether there is a transition cyst organization between one-to-one type and many-to-one type for cyst-forming myxosporean and the occurring mechanism of different types of cysts awaits further research.

Although most of myxozoans are not harmful to their host fish, *T. wangi*. n. sp. should be paid sufficient attention as an important pathogenic agent, for its cysts occupy or displace large respiratory area in fish gills and general high infection intensity (up to 30 cysts per fish in maximum). Furthermore, high density culture is common for nursing allogynogenetic gibel carp fry in China. So, the infection of *T. wangi*. n. sp. can cause mass mortality of nursed fry for hypoxia, especially under the condition of low DO although no significant inflammatory can be found based on our histopathological analysis. To date, no commercially chemotherapeutants and vaccines are available to copy with myxosporean infections, and the current myxosporidiosis control can only be depended on the biology of myxozoans (Yokoyama et al. 2012; Xi et al. 2013). Our investigation data showed that the development of *T. wangi*. n. sp. into mature myxospores and the formation of visible cysts from initial infection by possible actinospores were very quick (less than one month) compared with other Myxobolidae species, like *T. wuhanensis* (authors' unpublished data). Thus, it provides a possibility to control this myxosporidiosis by monitoring the actinospore dynamics in water column of the culture ponds and then applying some chemical reagents to kill or inactivate the infective actinospores in a short period. The elucidation of the full life cycles of *T. wangi*. n. sp. will not only help develop possible control strategies for this myxosporidiosis of allogynogenetic gibel carp by preventing from the completion of the life cycle in cultured pond ecosystem but also help enrich the study of life cycle of *Thelohanellus* spp., for only two species (*T. hovorkai* and *T. nikolskii*) are so far known to involve actinospores in their invertebrate host (Székely et al. 1998). In addition, taking into account that *Trichodina nobilis* is ubiquitous and of low prevalence and infection intensity, we speculated that there is no correlation of the infection of these two parasites.

Acknowledgments The present work was financially supported by the Jiangsu Province Fund of Sciences (BK2012240, BK2011182), Special Fund for Basic Scientific Research of Central Institutes, FFRC (6-115080), Young Scientist Award of the Knowledge Innovation Program of the Chinese Academy of Sciences, and Huai'an Science and Technology Bureau (SN12099, SN13095).

References

Abdel-Ghaffar F, Morsy K, Bashtar AR, El-Ganainy S, Gamal S (2013) *Thelohanellus niloticus* sp. nov. (Myxozoa: Myxosporea), a parasite of the Nile carp *Labeo niloticus* from the River Nile, Egypt. Parasitol Res 112:379–383

Adriano EA, Carriero MM, Maia AAM, Silva MRM, Naldoni J, Ceccarelli PS, Arana S (2012) Phylogenetic and host–parasite relationship analysis of *Henneguya multiplasmodialis* n. sp. infecting *Pseudoplatystoma* spp. in Brazilian Pantanal wetland. Vet Parasitol 185:110–120

Azevedo C, Samuel N, Saveia AP, Delgado F, Casal G (2011) Light and electron microscopical data on the spores of *Thelohanellus rhabdalestus* n. sp. (Myxozoa: Myxosporea), a parasite of a freshwater fish from the Kwanza River, Angola. Syst Parasitol 78:19–25

Bartosova P, Fiala I, Hypsa V (2009) Concatenated SSU and LSU rDNA data confirm the main evolutionary trends within myxosporeans (Myxozoa: Myxosporea) and provide an effective tool for their molecular phylogenetics. Mol Phylogenet Evol 53:81–93

Chen QL, Ma CL (1998) Myxozoa: Myxosporea. Science Press, Beijing

Fiala I (2006) The phylogeny of Myxosporea (Myxozoa) based on small subunit ribosomal RNA gene analysis. Int J Parasitol 36:1521–1534

Griffin MJ, Goodwin AE (2011) *Thelohanellus toyamai* (Syn. *Myxobolus toyamai*) infecting the gills of koi *Cyprinuscarpio* in the Eastern United States. J Parasitol 97:493–502

Gui JF, Zhou L (2010) Genetic basis and breeding application of clonal diversity and dual reproduction modes in polyploidy *Carassius auratus gibelio*. Sci China Life Sci 53:409–415

Guindon S, Dufayard JF, Lefort V, Anisimova M, Hordijk W, Gascuel O (2010) New algorithms and methods to estimate maximum-likelihood phylogenies: assessing the performance of PhyML 3.0. Syst Biol 59:307–321

Kent ML, Andree KB, Bartholomew JL, El-Matbouli M, Desser SS et al (2001) Recent advances in our knowledge of the Myxozoa. J Eukaryot Microbiol 48:395–413

Kimura M (1980) A simple method for estimating evolutionary rates of base substitutions through comparative studies of nucleotide sequences. J Mol Evol 16:111–120

Liu Y, Whipps CM, Gu ZM, Zeng C, Huang MJ (2012) *Myxobolus honghuensis* n. sp. (Myxosporea: Bivalvulida) parasitizing the pharynx of allogynogenetic gibel carp *Carassius auratus gibelio* (Bloch) from Honghu Lake, China. Parasitol Res 110:1331–1336

Liu Y, Jia L, Huang MJ, Gu ZM (2014a) *Thelohanellus testudineus* n. sp. (Myxosporea: Bivalvulida) infecting the skin of allogynogenetic gibel carp *Carassius auratus gibelio* (Bloch) in China. J Fish Dis 37:535–542

Liu Y, Yuan JF, Jia L, Huang MJ, Zhou ZG, Gu ZM (2014b) Supplemental description of *Thelohanellus wuhanensis* Xiao & Chen, 1993 (Myxozoa: Myxosporea) infecting the skin of *Carassius auratus gibelio* (Bloch): ultrastructural and histological data. Parasitol Int 63:489–491

Lom J, Arthur JR (1989) A guideline for preparation of species descriptions in Myxosporea. J Fish Dis 12:151–156

Lom J, Dyková I (2006) Myxozoan genera: definition and notes on taxonomy, life-cycle terminology and pathogenic species. Folia Parasitol 53:1–36

Luo YZ, Lin L, Wu ZX, Liu Y, Gu ZM, Li LJ, Yuan JF (2013) Haematopoietic necrosis of cultured Prussian carp, *Carassius gibelio* (Bloch), associated with Cyprinid herpesvirus 2. J Fish Dis 36:1035–1039

Molnár K (2002) Site preference of fish myxosporeans in the gill. Dis Aquat Organ 48:197–207

Page RDM (1996) TreeView: an application to display phylogenetic trees on personal computers. Comput Appl Biosci 12:357–358

Posada D (2008) JModelTest: phylogenetic model averaging. Mol Biol Evol 25:1253–1256

Shin SP, Nguyen VG, Jeong JM, Jun JW, Kim JH, Han JE, Baeck GW, Park SC (2014) The phylogenetic study of *Thelohanellus* species (Myxosporea) in relation to host specificity and infection site tropism. Mol Phylogenet Evol 72:31–34

Suo D, Zhao YJ (2010) Morphological redescription of *Thelohanellus nikolskii* Achmerov, 1955 (Myxozoa, Bivalvulida) and phylogenetic analysis of *Thelohanellus nikolskii* inferred from 18S rDNA. Acta Zootax Sin 35:90–95

Swofford DL (2003) PAUP*. Phylogenetic analysis using parsimony (* and other methods), v. 4.0 beta 10. Sinauer Associates, Sunderland

Székely C, El-Mansy A, Molnár K, Baska F (1998) Development of *Thelohanellus hovorkai* and *Thelohanellus nikolskii* (Myxosporea: Myxozoa) in oligochaete alternate hosts. Fish Pathol 33:107–114

Székely C, Shaharom-Harrison F, Cech G, Mohamed K, Molnár K (2009) Myxozoan pathogens of Malaysian fishes cultured in ponds and net-cages. Dis Aquat Org 83:49–57

Tamura K, Peterson D, Peterson N, Stecher G, Nei M, Kumar S (2011) MEGA5: molecular evolutionary genetics analysis using maximum likelihood, evolutionary distance and maximum parsimony methods. Mol Biol Evol 28:2731–2739

Thompson JD, Gibson TJ, Plewniak F, Jeanmougin F, Higgins DG (1997) The CLUSTRAL-X windows interface: flexible strategies for multiple sequence alignment aided by quality analysis tools. Nucleic Acids Res 24:4876–4882

Wang GT, Yao WJ, Wang JG, Lu YS (2001) Occurrence of thelohanellosis caused by *Thelohanellus wuhanensis* (Myxosporea) in juvenile allogynogenetic silver crucian carp, *Carassius auratus gibelio* (Bloch), with an observation on the efficacy of fumagillin as a therapeutant. J Fish Dis 4:57–60

Wang ZW, Zhu HP, Wang D, Jiang FF, Zhou L, Gui JF (2011) A novel nucleo-cytoplasmic hybrid clone formed via androgenesis in polyploidy gibel carp. BMC Res Notes 4:82

Xi BW, Xie J, Zhou QL, Pan LK, Ge XP (2011) Mass mortality of pond-reared *Carassius gibelio* caused by *Myxobolus ampullicapsulatus* in China. Dis Aquat Org 93:257–260

Xi BW, Zhang JY, Xie J, Pan LK, Xu P, Ge XP (2013) Three actinosporean types (Myxozoa) from the oligochaete *Branchirua sowerbyi* in China. Parasitol Res 112:1575–1582

Xiao CH (1988) Study of epidemiology and myxosporean fauna from silver crucian carp (*Carassius auratus gibelio* Bloch) (in Chinese with English summary). Master dissertation, Institute of Hydrobiology, Chinese Academy of Sciences

Ye LT, Li WX, Wang WW, Wu SG, Wang GT (2014) Updated morphology, histopathology and molecular phylogeny of *Myxobolus hearti*, cardiac myxosporea in gibel carp, *Carassius gibelio* (Bloch). J Fish Dis 37:11–20

Yokoyama H, Liyanage YS, Sugai A, Wakabayashi H (1998) Hemorrhagic thelohanellosis of color carp caused by *Thelohanellus hovorkai* (Myxozoa: Myxosporea). Fish Pathol 33:85–89

Yokoyama H, Grabner D, Shirakashi S (2012) Transmission biology of the myxozoa, health and environment in aquaculture. In: Carvalho E (ed) InTech, Available from: http://www.intechopen.com/books/health-and-environment-in-aquaculture/transmission-biology-of-the-myxozoa

Zhang JY, Wang JG, Li AH, Gong XN, Cai TZ (2006) Redescription of *Myxobolus pyramidis* Chen, 1958 (Myxosporea: Bivalvulida). Parasitol Res 99:65–69

Zhang JY, Wang JG, Li AH, Gong XN (2010a) Infection of *Myxobolus turpisrotundus* n. sp. in allogynogenetic gibel carp, *Carassius auratus gibelio* (Bloch), with revision of *Myxobolus rotundus* (s. l.) Nemeczek reported from *C. auratus auratus* (L.). J Fish Dis 33:625–638

Zhang JY, Yokoyama H, Wang JG, Li AH, Gong XN, Ryu-hasegawa A, Iwashita M, Ogawa K (2010b) Utilization of tissue habitats by *Myxobolus wulii* Landsberg and Lom, 1991 in different carp hosts and disease resistance in allogynogenetic gibel carp: redescription of *M. wulii* from China and Japan. J Fish Dis 33:57–68

Zhang JY, Gu ZM, Kalavati C, Eiras JC, Liu Y, Guo QY, Molnár K (2013) Synopsis of the species of *Thelohanellus* Kudo, 1933 (Myxozoa: Myxosporea: Bivalvulida). Syst Parasitol 86:235–256

Zhao YJ, Sun CY, Kent ML, Deng JL, Whipps CM (2008) Description of a new species of *Myxobolus* (Myxozoa: Myxobolidae) based on morphological and molecular data. J Parasitol 94:737–742

Zhao YJ, Zhao YJ, Li NN, Tang FH, Dong JL (2013) Remarks on the validity of Myxobolus ampullicapsulatus and Myxobolus honghuensis (Myxozoa: Myxosporea) based on SSU rDNA sequences. Parasitol Res 112: 3817–3823

Zhu YT, Lu HD, Cai SJ (2012) Redescription of *Thelohanellus wuhanensis* Xiao et Chen (Myxozoa, Myxosporea) infecting allogynogenetic crucian carp (*Carassius auratus gibelio*) and phylogenetic analysis based on 18S rDNA sequence. Acta Zootax Sin 37:681–686